

Effect of Biomass Type, Pyrolysis Temperature and Pressure on Agronomic Properties of Biochar

Gizem Balmuk^a, María Videgain^b, Joan J. Manyà^b, Gozde Duman^c, Jale Yanik^{c,*}

^a *Center for Environmental Studies, Ege University, Izmir 35100, Turkey.*

^b *Aragón Institute of Engineering Research (I3A), Thermochemical Processes Group, University of Zaragoza, Escuela Politécnica Superior, Crta. de Cuarte s/n, 22071 Huesca; Spain.*

^c *Faculty of Science, Department of Chemistry, Ege University, 35100 Izmir, Turkey.*

ABSTRACT

This study focused on identifying the effect of pyrolysis temperature and pressure for lignocellulosic biomass on agronomic properties of biochar. For this purpose, two biomasses (vine shoots -VS and corn stover -CS) were pyrolyzed at different temperatures (350 and 500 °C) under different pressures (0.1 and 0.5 MPa) for a residence time of 60 min. Agronomic properties of biochars (including stability, pH, CEC, EC, bulk density, surface properties, and water holding capacity) were determined. Pyrolysis temperature impacted greatly on the biochar stability and the textural properties. The dependence of other properties of biochars on pressure and temperature varied as a function of the type of feedstock. In addition, the effects of pyrolysis temperature and pressure on 16 US EPA PAH concentration in biochar were also investigated. The PAH concentrations ranged between 0.822 and 5.112 mg kg⁻¹. On average, VS-derived biochar had higher PAH concentrations than CS-derived one. The structural differences in biomass played a key role in determining the effect of pyrolysis conditions on total PAH concentration.

1. Introduction

Biochar, a C-rich solid material, is produced mostly by pyrolysis of biomass in an oxygen depleted environment. The interest in biochar, which was first seen as a tool for carbon sequestration in soil, soon turned into a focus on the agricultural and environmental remediation potential. Besides enhancing soil organic carbon sequestration and mitigating greenhouse gas (GHG) emissions, biochar improves soil productivity [1] and immobilize contamination from soil [2]. Biochar is a highly heterogeneous material, and its properties vary widely depending on both the nature of the raw material and production conditions. The number of reported biochar studies has increased rapidly since 2010 [3]. In these studies, versatile properties of biochars are mostly pointed out, which enhance the soil fertility in multiple ways. Biochar

contains considerable amount of micro and macronutrients (such as K, Ca, P, Mg, NH₄-N/NO₃-N, Zn, and Fe), which are essential for plant growth. Owing its porous structure and relatively high surface area, addition of biochar into soil stimulates microbial activity. Functional groups on the surface of biochars can also reduce nutrient leaching [4–6].

Despite the potential benefits of biochar, there are conflicting results in the literature regarding the effect of biochar on soil quality [7]. The potential environmental risks and negative impacts on nutrient availability related to biochar applications have been reported in the literature [8]. Depending on biomass source and pyrolysis conditions, biochar may act as a carrier of toxic compounds, namely heavy metals and polyaromatic hydrocarbons (PAH). The latter is particularly hazardous for both human health and plant growth and its degradation is difficult due to its recalcitrant structure. PAH compounds are formed during pyrolysis depending on process conditions as well as biomass type; therefore, reducing PAH content in biochar can be possible by fine tuning pyrolysis process conditions. Despite the numerous studies already reported on the impact of raw material and pyrolysis temperature on the physicochemical properties of resulting biochars [3,9], to the best of our knowledge, no attention has been paid to the role of pyrolysis pressure on the agronomic properties of biochar. In this study, biochars were produced at two pyrolysis temperatures and pressures from two agricultural residues, vine shoots and corn stover. The novelty of this study is the investigation of the effects of process pressure on the agronomic properties of biochar. Due to the pyrolysis conditions and raw material-specific nature of biochars, this study provides an insight in the direction of “engineered biochars”.

2. Materials Methods

2.1. Materials

In this study, two agricultural wastes, vine shoots (VS) and corn stover (CS) were used. Vine shoots (having 8.5–15 mm diameter) were collected in the wine region of Somontano (Huesca province, Spain). Corn stover consisting of a mixture of corncob (15.4 wt%), leaf (80.1 wt %), and stalk (4.5 wt%) was collected in a field located in the province of Huesca (Spain). Vine shoots were cut into smaller pieces of 4–7 cm in length, whereas particle sizes of corn leaves were 14–16 cm in length and 1.0–2.0 mm in thickness. Some properties of agricultural wastes are given in Table S1 (supplementary material). Their lignocellulosic component contents, which were analyzed following a method described in a previous study [10], are quite different from each other. VS had a considerably higher lignin content than CS.

2.2. Pyrolysis

Pyrolysis experiments were carried out in a fixed bed design and stainless steel reactor (140 mm ID and 465 mm long). More details regarding the configuration of the pyrolysis system are available in a previous study [10]. In a typical run, 300 g for VS and 130 g for CS, was placed into the reactor. The system was heated up to desired temperature at an average heating rate of $5\text{ }^{\circ}\text{C min}^{-1}$, and held for 60 min. A back-pressure regulator was used to maintain the pressure of the pyrolysis reactor at a desired value (0.1 and 0.5 MPa). Nitrogen flow was adjusted at a flow rate of 6.48 L min^{-1} , corresponding to a carrier gas residence time of 150 s within the reactor (at the corresponding pressure and peak temperature). After pyrolysis, the reactor was cooled down to room temperature in nitrogen atmosphere. The solid product in reactor was collected and weighed in order to calculate the biochar yield.

2.3. Characterization

The elemental analysis of agricultural wastes and biochars were carried out using a CHNS analyzer (LECO) according to ASTM D5373–16. The ash and volatile matter contents were measured following ASTM standard D1762–84. The inorganic constituents of the agricultural waste ashes were determined by X-ray fluorescence (XRF) spectroscopy according to ASTM D4326–04. Specific surface areas (S_{BET}) were determined from the CO_2 adsorption isotherms at $0\text{ }^{\circ}\text{C}$ (using an ASAP 2020 adsorption analyzer from Micromeritics). The morphology of biochars was identified by Scanning electron microscopy (SEM) images taken at various magnitudes by Thermo Scientific Apreo S microscope. Prior to analysis, biochars were coated with gold for providing the necessary conductivity for high image quality. Bulk density was calculated using the mass of biochar that could be packed into a 25 mL glass cylinder with minimal compression [11]. For the pH and electrical conductivity (EC) measurement, biochar samples were suspended in deionized water in a 1:10 (wt./wt.) ratio. After 24 h of stirring, pH and EC of solution were measured using a pH electrode and a conductivity electrode, respectively. For determination of water extractables, biochar samples were also suspended in deionized water at the same ratio as reported before and stirred during 24 h. The suspension was centrifuged and then supernatant was filtered prior to further measurements. Na^+ and K^+ concentrations in supernatant were determined using a flame photometer. Ca^{2+} and Mg^{2+} concentrations were determined by ICP/MS. $\text{NH}_4\text{-N}$ and $\text{NO}_3\text{-N}$ concentrations were colorimetrically determined according to Phenate-EPA colorimetric method and Brucine test method, respectively. The cation exchange capacity (CEC) of biochars was determined by the ammonium acetate (NH_4OAC) extraction methods and following Phenate colorimetric method

[12]. The unstable organic C was determined by potassium dichromate method [12]. The stable organic carbon was calculated by the difference between the total organic carbon content and unstable organic carbon content of biochar. To characterize the biochar functional groups, the infrared spectrum of biochars (working range 400–4000 cm^{-1} , resolution 4 cm^{-1}) was recorded using a Perkin Elmer FTIR coupled with attenuated total reflectance (ATR).

Water holding capacity (WHC) of biochars was determined according to DIN EN ISO 14238. To determine the amounts of PAH contained in the chars, biochar sample (1–3 g) was transferred into a glass tube, and 20 mL of acetone/cyclohexane (1:1, v/v) were added. PAH surrogate (containing naphthalene-d8, acenaphthene-d10, phenanthrene-d10, chrysene-d12, perylene-d12) was spiked into the mixture to calculate the extraction recoveries. The mixture was left for overnight and then ultrasonicated for 30 min. After solution was filtered to remove biochars particles, solution was first concentrated by using nitrogen gas and subjected to solvent exchange. Cleaning (Agilent Bond Elute) column was used to remove contaminants in extracted sample, which may interfere with PAH during analysis. GC-MS analyses were performed using a 6850 Agilent HP gas chromatograph coupled with quadrupole mass spectrometer. Analytes were separated by a HP-5MS capillary (30 m \times 0.25 mm \times 0.25 μm), using helium as the carrier gas. The following thermal program was used: capillary column was hold at 50 $^{\circ}\text{C}$ for 1 min, from 50 $^{\circ}\text{C}$ to 200 $^{\circ}\text{C}$ with a heating rate of 25 $^{\circ}\text{C min}^{-1}$ and from 200 to 300 $^{\circ}\text{C}$ at a heating rate of 8 $^{\circ}\text{C min}^{-1}$, then a hold for 5.5 min at 300 $^{\circ}\text{C}$. The temperatures of the injector, ion source and quadrupole were 295, 300, and 180 $^{\circ}\text{C}$, respectively. The mass spectrometer operated under electron ionization (70 eV) and acquisition was performed on single ion monitoring (SIM).

3. Results

3.1. Yield and stability of biochars

The agricultural wastes and biochars used in this study have been characterized in our previous study [10]. To evaluate the effect of pyrolysis temperature and pressure on agronomic characteristics of biochars obtained from two different temperature and two different pressure was investigated. The biochars were denoted as following the “Biomass type - Process Temperature - Process Pressure” sequence. The yield and basic properties of biochars are given in Table 1.

As expected, the increase in the pyrolysis temperature led to a decrease in both biochar yield as well as H/C and O/C ratios. On the other hand, pressure had marginal effect on the biochar

yield. Regarding the pressure effect on H/C and O/C, it is not easy to reach a common consensus (varied depending on the feedstock composition and pyrolysis temperature).

Biochar is not completely inert material in soil, but its mineralization by soil microorganisms is extremely slow. The O/C ratio has important implications on biochars stability [13]. Generally, it is assumed that biochars with an atomic O/C ratio below 0.2 have a half-life greater than 1000 years, whereas O/C ratios in the range of 0.2–0.6 have half-lives between 100 and 1000 years. [14]. H/C ratio is also an indicator, the carbonized organic matter with a H/C ratio lower than 0.7 is defined as biochar by IBI and EBC. Obviously and in agreement with earlier studies [15,16], high temperature pyrolysis produces more stable biochar than low temperature.

Table 1 Yields and properties of biochars [10].

	Yield, %	Ash, %	VM, %	Ultimate Analysis, % (db)				O:C (atomic)	H:C (atomic)
				C	H	N	O		
VS-350-0.1	42.7	7.5	40.8	76.6	5.36	2.17	8.42	0.08	0.84
VS-350-0.5	40.1	6.3	39.2	75.7	5.73	2.19	10.1	0.10	0.91
VS-500-0.1	34.2	5.8	22.2	83.3	3.97	2.28	4.64	0.04	0.57
VS-500-0.5	33.2	6.4	20.7	84.4	3.70	2.41	3.09	0.03	0.53
CS-350-0.1	49.7	5.2	42.4	68.5	4.78	1.14	20.4	0.22	0.84
CS-350-0.5	37.4	4.4	42.1	70.1	4.48	1.39	19.6	0.21	0.77
CS-500-0.1	27.1	8.4	21.9	78.5	3.10	1.57	8.47	0.08	0.47
CS-500-0.1	30.1	7.8	24.4	73.7	3.23	1.45	13.8	0.14	0.53

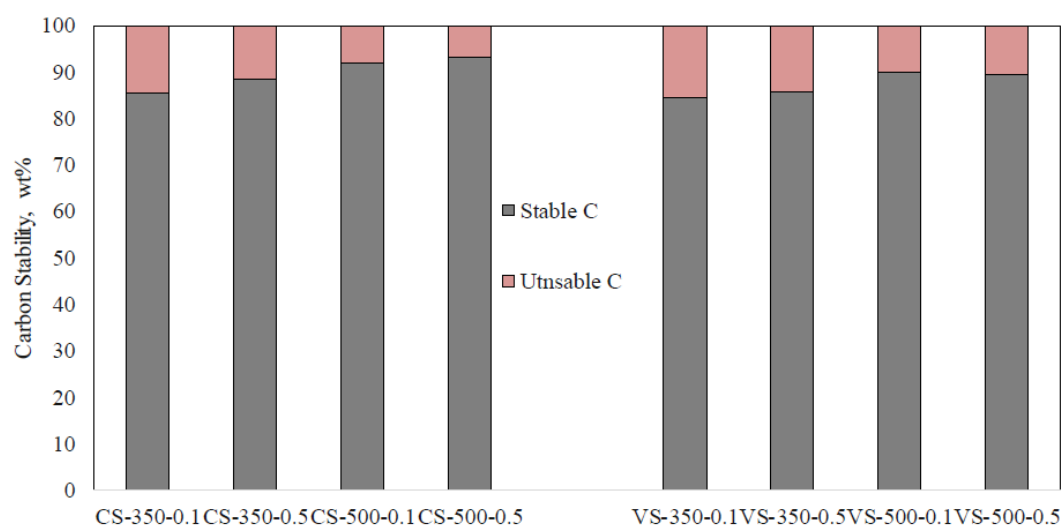


Fig. 1. Percentages of stable/labile organic carbon in biochars.

According to EBC guidelines, biochar with a H/C ratio lower than 0.7 and an O/C ratio below 0.4 is stable; therefore, samples VS-500–0.1, VS-500–0.5, OS-500–0.1 and OS-500–0.5, which met the two criteria, could be categorized as stable. The stability of biochar should also be evaluated in terms of the labile and stable fraction of C in biochar [17]. The percentages of stable C in CS-derived biochars were in the range of 85.4% and 93.2%, whereas they were in the range of 84.6% and 89.3% for VS-derived biochars (see Fig. 1). As seen in Fig. 1, high pyrolysis temperature increased the stable fraction of C in biochar. The effect of pressure on the percentages of stable C was observed only for CS-derived biochars produced at 350 °C. The stable fraction of C in the biochar slightly increased from 84.4% to 88.4% when the pyrolysis pressure raised from 0.1 to 0.5 MPa.

The main benefit of biochar to soil quality and to environment is increased storage of organic C. If biochar is considered for soil carbon sequestration, then it is desirable to have maximum stable C. However, if biochar is considered for microbe's food source for increasing soil nutrients availability, water holding capacity and biochar based controlled release fertilizers, the release of certain labile C may be beneficial. [18]. Furthermore, the labile C fraction in biochar has significant effects on N mineralization or immobilization in soil [13], and on the promotion of the soil microbial activity by labile C substrates [9]. The ash fraction of biochars consists of the minerals contained in the original feedstock (see Table S2). As the minerals in feedstock largely remains during pyrolysis, the concentrations of elements such as P, K, Ca, and Mg increased in biochars.

3.2 Fourier transform infrared spectroscopy analysis

The functional groups of biochars were characterized by ATR-FTIR, and the spectra were displayed in Fig. 2. Regardless of the biomass type and pressure, the intensity of peak around 1695 cm^{-1} , which is associated with C=O stretching of aldehyde, ketone and other carbonyl acid, decreased with increasing the pyrolysis temperature from 350 to 500 °C. For CS-derived biochars, the peak at 1600 cm^{-1} (aromatic C=C ring stretching) was observed for all samples; however, the intensity of which varied with pyrolysis temperature. With increase of pyrolysis temperature, aromatic C=C stretching peak was more pronounced while the intensity of carbonyl peak at 1695 cm^{-1} decreased. In the case of CS-350–0.1, the peaks at 1050 cm^{-1} and 1160 cm^{-1} , which are associated with C–O and C–O–C groups respectively, weakened at higher pressure and temperature. One can be concluded that decarboxylation/decarbonylation and aromatization reactions took place at higher temperature, resulting in reduction of carboxylic

groups and formation of aromatic structure in biochar. It was also reported that aliphatic and aromatic carboxylic acids in biochar tend to cause phytotoxicity [12].

In case of VS, small peak around 1320 cm^{-1} , which is assigned to C–O stretching, was observed in only low temperature biochars (VS-350–0.1 and VS-350–0.5). The peak around $1410\text{--}1430\text{ cm}^{-1}$, which is associated with C–H in-plane bending of –C=C–H groups, was observed in all VS-derived biochars, noting that the intensity was low in case of VS-350–01. Differently in low temperature biochars, C–H out of plane vibration peak at 870 cm^{-1} indicated the presence of aromatic structure in high temperature biochars. Comparing to CS-derived biochars, C–O stretching peak (at 1050 cm^{-1}) was not observed in VS-derived biochars. This is probably related to the lower O content and O/C ratios measured for biochars produced from vine shoots.

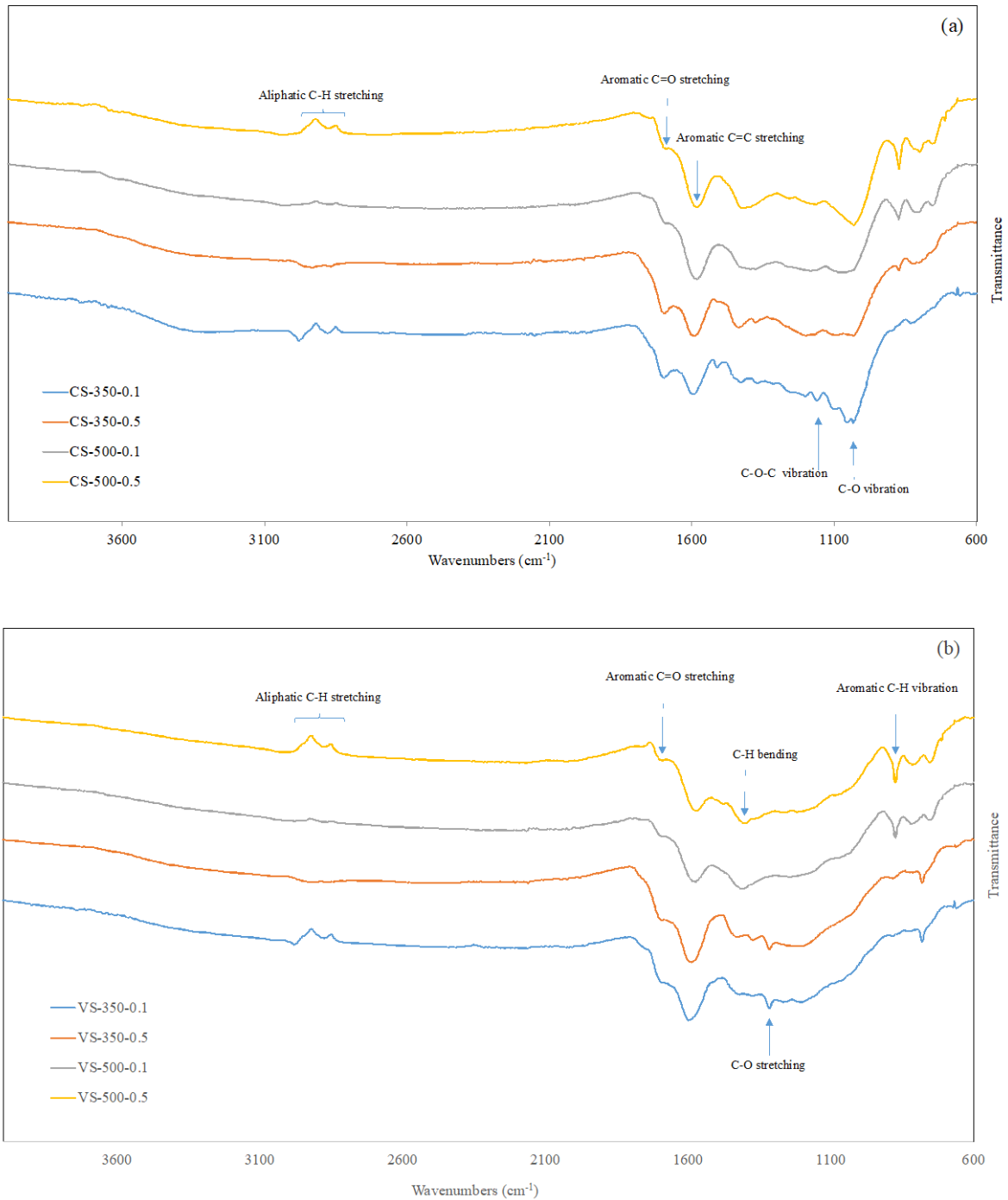


Fig. 2. FTIR spectra of biochar samples.

3.3 Physical characterization of biochar

As known, the physical properties of biochar affect its mobility in the environment, interaction with soil water, nutrients and suitability as an ecological niche for microbial colonization. Bulk density is important in materials handling and application. It would be to point out that density is not an intrinsic property of the material, but it depends on the size, shape and compaction of the particles. Generally, biochars have a bulk density ranging from 0.06 to 0.7 g cm⁻³.

In this study, biomass source was found to be the most important factor in the bulk density of biochar rather than pressure and temperature (see Table 2). Although Das et al. [9] found that biochar bulk density positively correlated with ash content and total carbon content of biochar, there was no significant correlation in our study. CS-derived biochars are denser than VS-derived biochars, which may be due to the higher silicon compounds in CS (Table S1).

The surface areas and pore volumes of biochars were determined from the CO₂ adsorption isotherms, instead of N₂ adsorption isotherms, due to the highly microporous structure of biomass-derived pyrolysis chars [19]. The surface area and porosity of biochar are important in soil remediation. They are determinative of the active sites amount, and thereby improving cation exchange capacity, water holding capacity and adsorption capacity [20]. In addition, the pores of biochar play a role as the habitat and refuge for soil microorganisms, which promote plant growth. SEM images presented in Fig. 3 illustrate the morphologies of the biochars prepared under different temperature and pressure. The pyrolysis pressure at 350 °C did not change the structure of biochars obtained from CS and VS. On the other hand, increase of pyrolysis temperature at atmospheric pressure led to form spherical voids created by release of the volatile matter. Particularly, SEM images of CS type biochars clearly revealed that biochar underwent morphological changes at higher temperatures, ending up a structure with perforated surface. The SEM results were in agreement with the BET results. For both biomasses, biochars produced at 500 °C had much higher surface area than biochars produced at 350 °C. Similarly, a dramatic increase in surface area and total pore volume in the 300–500 °C range have been observed in previous study due to the enhanced volatilization.[20]. The increase in pyrolysis pressure did not have a considerable influence the textural properties (porosity, S_{BET} and V_{ultra}) of biochars.

Table 2 Physical properties of biochars.

	Bulk density, g/cm ³	WHC, %	S _{BET} , m ² g ⁻¹	V _{ultra} , cm ³ g ⁻¹
VS-350-0.1	0.15	234	134	0.035
VS-350-0.5	0.12	78	127	0.029
VS-500-0.1	0.14	225	208	0.064
VS-500-0.5	0.15	129	217	0.069
CS-350-0.1	0.32	114	123	0.027
CS-350-0.5	0.34	114	143	0.032
CS-500-0.1	0.31	103	215	0.067
CS-500-0.5	0.30	98	211	0.062

Contrary to our result, in fast pyrolysis of pine at 900 °C, the CO₂ surface area of biochar showed a constantly decreasing trend (from 476 to 349 m² g⁻¹) as the increasing pressure from 1 to 20 bar [21]. Similarly, Melligan et al. [22] studied the slow pyrolysis of Miscanthus at 550 °C and reported significant differences in the surface area of the biochar produced at different pressures. The surface area of biochar produced at atmospheric pressure (161.7 m² g⁻¹) decreased rapidly as the pressure was increased (for 2, 6 and 26 bar the N₂ surface area was 15.85, 2.26 and 0.14 m² g⁻¹, respectively). They suggested that the surface area decreased because the high-pressure during pyrolysis led to the trapping of tar on the surface and also the collapse of the pore structures. The apparently contradictory results obtained in the present study could be explained by the fact that the reaction parameters (temperature, heating rate and residence time) and biomass properties (particle size, shape and structure) are different from those in other studies. Overall, the surface areas of biochars obtained at 500 °C are comparable to the surface areas of biochars derived from herbaceous and agricultural biomass with the same pyrolysis temperature in literature [20].

Regarding the water holding capacities of biochars, we obtained fundamentally different results: WHC was dependent on pyrolysis pressure in the case of VS-derived biochars; however, neither pressure nor temperature of pyrolysis did not affect WHC of CS-derived biochars. WHC of VS-derived biochars was higher compared to CS-derived biochars and higher WHC for low pressure compared to high pressure.

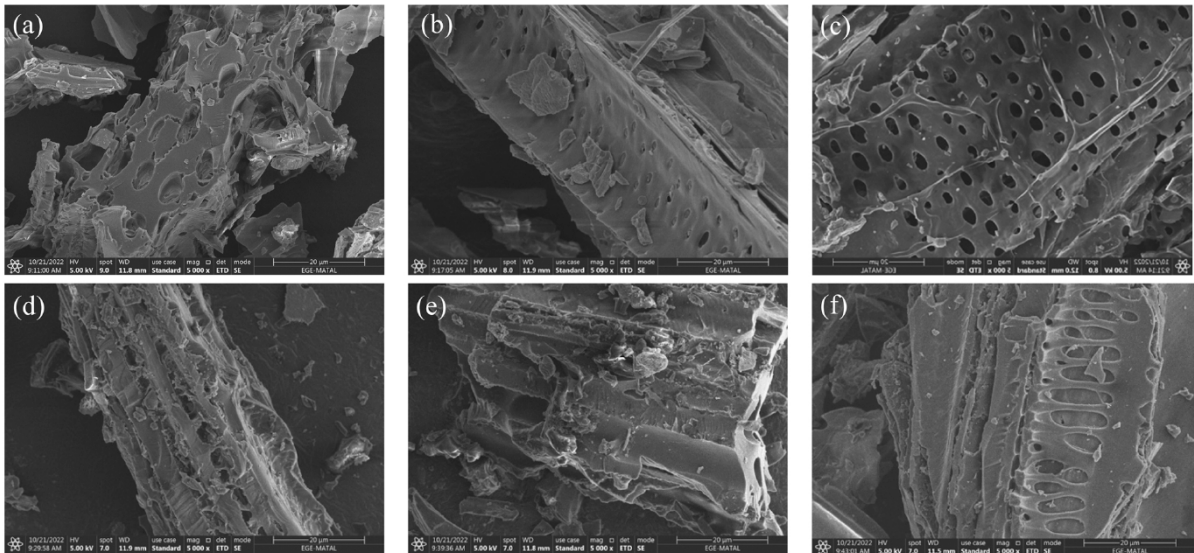


Fig. 3. SEM photos of biochars at various temperatures and pressures: (a)CS-350–0.1, (b)CS-350–0.5, (c)CS-500–0.1, (d)VS-350–0.1, (e)VS-350–0.5, (f)VS-500–0.1.

3.4 pH, CEC and EC of biochars

Due to its alkaline characteristic, acidic soil pH can be regulated by biochar applications on soil. The pH values of biochars are primarily correlated with the contents of inorganic alkalis. Increased pH with an increase in pyrolysis temperature is associated with the increase in ash content and separation of alkali salts from the organic matrix [23]. In addition, the disappearance of acidic functional groups and appearance of basic functional groups have been reported to increase with increasing temperature, contributing to further increase the pH of resulting biochars [24]. In line with the results available in the literature, pH of VS-derived biochars increased with pyrolysis temperature (see Table 3), although the ash content of the biochars did not change significantly. In contrast, the pH of CS-derived biochars did not change significantly with pyrolysis temperature even their ash contents increased. This may be attributed to its ash composition, lower alkali salt contents than that of CS-derived biochars. VS-500–0.1 and VS-500–0.5 with high liming potential can contribute to soil productivity by adjusting low pH of acidic soils. The other biochars having neutral pH value are favorable to use in many soils (both acidic and alkaline). It should be mentioned that the effect of biochar on soil pH depends on the application rate [25], as well as pH of biochar.

Cation exchange capacity (CEC) is an important parameter to assess the effect of biochar on soil properties. CEC is an indication of ability to adsorb soil nutrients such as Ca, Mg, K, Na and NH_4 . Glaser et al. [26] stated that anthropogenic soil in Amazon Forest had high CEC value and fertility due to the presence of pyrogenic carbon, which is mainly produced after plant and

forest fires. Recent studies showed that CEC values of biochars varied with production conditions such as pyrolysis temperature, feedstocks, retention times, etc. [27]. CEC values of biochars were found to be 20.1–75.8 cmol kg⁻¹, which are close to those obtained from different biomass in our previous work [28]. It was previously reported that CEC of biochars could be positively correlated with oxygen functional groups having a negative charge in basic and neutral solutions, which is electrostatically attracted to cations [29]. For both VS- and CS-derived biochars, higher pyrolysis temperature resulted in lower CEC values due to the loss of surface oxygen functional groups at high temperatures. FTIR results also support this idea (Fig. 2), as a decrease in C=O stretching with increasing the pyrolysis temperature from 350 to 500 °C was observed. Strong correlation between O/C ratio and CEC value was also reported in previous studies [30,31]. In this study, the biochars with higher O/C ratio gave higher CEC value for identical biomass precursor. In addition, Lehmann et al. [32] stated that volatile matter including organic acids increased the amount of negative charge in biochars, leading to an improved CEC value. We also observed that volatile content of biochar strongly affected the CEC values; the higher volatile content, the higher CEC value. Nonetheless, it should be noted that in case of VS-derived biochars, the CEC values of biochars having almost similar volatile content and O/C ratios are not identical. This result suggests that CEC value cannot be associated only with volatile matter content and O/C ratio.

Table 3 pH, EC and CEC values of biochars.

	pH	EC (dSm ⁻¹)	CEC (cmol kg ⁻¹)
VS-350-0.1	7.16	2.68	53.8
VS-350-0.5	7.13	2.89	75.8
VS-500-0.1	9.67	2.02	35.5
VS-500-0.5	8.86	1.44	20.1
CS-350-0.1	7.03	1.21	46.8
CS-350-0.5	7.34	1.16	45.2
CS-500-0.1	7.31	1.03	28.3
CS-500-0.5	7.29	0.91	32.3

Electrical conductivity (EC) value gives the estimation of the amount of soluble salts in a biochar solution and is an important index reflecting the ability as fertilizer. High rates of biochar application to soil may adversely affect salt sensitive plants, leading to water stress, salt stress and nutrient imbalances [33]. As in the case of pH, EC value of biochars varied to the

largest extent with pyrolysis temperature and type of biomass. EC of VS-derived biochars increased with pyrolysis temperature, while the pH of CS-derived biochars did not change significantly with pyrolysis temperature. In general, a substrate with an EC in the range of 0.5–1.5 dS m⁻¹ is considered moderately saline, 1.5–2.0 dS m⁻¹ extremely saline and above 2.0 dS m⁻¹ too saline (L). The results in Table 3 suggest that applying VS-derived biochars (except VS-500–0.5) may increase the soil salinity.

3.5 Water soluble nutrients

One of the agronomic benefits of biochar is that it may contain substantial amounts of plant nutrient elements. However, the agronomic effectiveness of these nutrients depends on their availability, which is related to several factors, being one of them the solubility of nutrients in water [34]. The water soluble nutrient contents of biochars are given in Table 4. As can be deduced from the table and in line with a previous study [35], pyrolysis temperature and feedstock type significantly affected nutrient concentrations and nutrient element speciation in biochar. The ammonium nitrogen (NH₄-N) and nitrate nitrogen (NO₃-N) are useful indicators to predict the agronomic effectiveness of biochar, since they are the main sources of available N for plant uptake. NO₃-N concentration in biochars derived CS was found to be less than NH₄-N concentration while opposite result was observed for biochars derived VS. A decrease in NH₄-N was observed with increasing temperature. The decrease in NH₄-N was due to the volatilization of the N-containing structures during heat treatment. It should be noted that the total amount of both type of nitrogen species decreased with increasing pressure for both biomass types. The reason might be conversion of the N-containing organics into insoluble N-heterocyclic aromatic structures by condensation reactions under pressure. The water soluble K concentration of the biochars slightly increased with increasing temperature, possibly due to separation of K salts from organic materials [28]. Overall, the decrease in the water solubility of alkaline in the biochars produced at high temperature could be explained by formation of insoluble minerals dominated by Ca and Mg.

Table 4 Water soluble nutrient contents, mg/kg.

	Mg	Ca	Na	K	NH ₄ -N	NO ₃ -N
VS-350-0.1	1631.59	2082.37	14.08	2716.69	41.85	700.21
VS-350-0.5	858.66	1690.22	15.85	4232.67	27.49	535.50
VS-500-0.1	365.38	357.00	10.54	2857.95	24.09	145.12
VS-500-0.5	85.35	201.51	16.93	4428.86	17.90	106.15
CS-350-0.1	261.04	658.06	53.28	1955.46	88.63	200.98
CS-350-0.5	250.66	656.47	39.32	1669.01	76.81	89.05
CS-500-0.1	73.92	299.24	29.25	2226.20	45.17	296.65
CS-500-0.5	95.83	406.57	19.74	1829.89	38.83	180.89

On the other hand, the increased pyrolysis pressure led to an overall decrease in water soluble nutrient contents in biochars, probably due to the enhanced formation of insoluble nutrient compounds. As an exception to the general trend, water soluble K content in VS-derived chars considerable increased with an increase in pyrolysis pressure. Further studies are required for better understanding the effect of pressure on the evolution of nutrient species during pyrolysis.

3.6 Concentration of PAHs in biochars

Although biochar has many agronomic benefits, it can be a potential risk for the environment due to its content in polycyclic aromatic hydrocarbons (PAHs). During pyrolysis of biomass, PAHs are formed by the recombination reactions and trapping of volatiles rich in PAHs leading to increase the abundance of PAHs in the biochar [36]. PAHs are formed by both Diels-Alder reactions at lower pyrolysis temperature and by condensation of phenol, alkyl-phenols and BTEX into larger compounds at temperatures above 400–500 °C [37]. The PAHs existing in biochar may enter ecosystems after being applied to the soil and threaten human health. The relationship between types/concentration of PAHs in biochar and pyrolysis conditions (biomass type, temperature, heating rate, gas flow type, reactor type etc.) still remain unclear. However, Buss et al., who investigated the effect of the temperature, residence time, carrier gas flow and biomass type for 46 biochars, concluded that it is possible to minimize PAHs concentration in biochar by combining properly feedstock with reactor design and operating parameters [38].

On the other hand, as far as we know, there is only one study investigating the effect of absolute pressure on PAH formation. Greco et al. observed a marked decrease in PAHs in wood waste-derived biochars by increasing pressure [37].

The individual concentrations and the sum of the 16 USEPA PAHs concentrations for selected biochars are given in Table 5. Extraction recoveries were found between 65% and 90%. The low-molecular weight PAHs (the sum of naphthalene, acenaphthylene, acenaphthene, fluorene and carbazole) were predominated in all biochars (except for CS-350–0.1). None of the produced biochars did not exceed the maximum permitted limit of 16 USEPA PAHs ($6.0 \pm 2.2 \text{ g t}^{-1}$) set by the European Biochar Certificate (EBC basic) (<https://www.european-biochar>). CS pyrolysis yielded biochar with much higher PAH concentrations than VS under identical pyrolysis conditions. This is because of the structural difference between the two biomasses. The lignin content of VS is higher than that of CS (see Table S1). As revealed in a previous study, in which the effect of interactions of biomass constituents on PAH was investigated, the formation of PAHs can be reduced due to interactions between xylan and lignin, while interactions between xylan and cellulose can result in a promoted PAH formation [39]. Besides the structural differences in biomasses, pyrolysis conditions can also affect the total PAH concentration. In the case of CS-derived biochars, total PAH concentration varied depending on both pressure and temperature. Conversely, the total PAH concentrations in biochars produced at both 350 and 500 °C were almost the same for VS-derived biochars. These apparently contradictory outcomes regarding the effect of pyrolysis temperature are in line with the existing literature. For instance, Freddo et al. [40] reported that PAHs contents of biochars produced at 300 °C from redwood, bamboo, rice straw and maize were higher compared to that of biochars produced at 600 °C. In contrast, Brown et al. [41] and Zielinska & Oleszczuk [42] reported the opposite trend: an increase in pyrolysis temperature led to an increase in PAH concentration in biochar. Buss et al. [38], who studied the effects of feedstock types (wood and straw) and pyrolysis temperature on PAHs content in the biochars, speculated that maximum yield of accumulated PAH on biochar increases up to a certain temperature and then decreases at higher temperatures due to the simultaneous formation and evaporation of PAHs from the biochar with increasing temperature. In their study, for biochars produced in the temperature range of 350–650 °C, they observed the highest PAH concentration in biochar produced from miscanthus chip at 450 °C, whereas this value was 550 °C for willow chips-derived biochar.

Regarding the effect of pressure on the contents of PAHs, it was observed a marked dependence on both the pyrolysis temperature and biomass type. For CS-derived biochars at low pyrolysis temperature (i.e., 350 °C), an increase in pressure led to a marked decrease in the concentration of total PAHs. Furthermore, low molecular weight PAHs in biochar produced at 0.5 MPa appeared to be more abundant than those at 0.1 MPa, while high molecular weight PAHs

showed the reverse pattern. At 350 °C, PAHs are formed from mainly degradation of hemicellulose and cellulose. As suggested by Zhou et al. [39], interaction of xylan and cellulose might enhance the PAH formation. However, pressure could inhibit the generation of PAHs by condensation and polymerization. On the other hand, at high temperature pyrolysis (e.g., 500 °C), pressurized pyrolysis led to a significant increase in PAHs concentration. The increase in PAHs concentration might be explained by a partial suppression of PAH vaporization at higher pressure. It should be kept in mind that the PAH concentration in the biochar is the difference between formed PAHs and evaporated PAHs [38]. The results obtained in this study differ from those Greco et al. [37], who observed that PAHs content in the biochars were significantly reduced by increasing either the peak temperature or the pressure, although their experiments were performed in identical pyrolysis conditions. These contradictory findings provide evidence that the type of feedstock plays a more determinant role than that of pyrolysis conditions on the formation and evolution of PAHs.

Table 5 Concentrations of the 16 USEPA priority polycyclic aromatic hydrocarbons, mg/kg.

	CS-350- 0.1	CS-350-0.5	CS-500- 0.1	CS-500- 0.5	VS-350- 0.5	VS-500- 0.5
Naphthalene	-	0.609	0.423	1.268	0.383	0.360
Acenaphthylene	0.297	0.088	0.017	0.368	0.017	0.015
Acenaphthene	0.162	0.040	0.012	0.072	0.005	0.005
Fluorene	0.256	0.133	0.022	0.513	0.030	0.035
Phenanthrene	0.700	0.307	0.130	1.117	0.191	0.187
Anthracene	0.065	0.038	0.013	0.287	0.015	0.017
Carbazole	0.279	0.071	0.030	0.587	0.030	0.028
fluoranthene	0.149	0.061	0.039	0.179	0.034	0.035
Pyrene	0.180	0.070	0.042	0.200	0.036	0.039
benzo[a]anthracene	0.006	0.036	0.018	0.066	0.012	0.015
Chrysene	0.255	0.158	0.038	0.345	0.034	0.048
benzo[b]fluoranthene	1.648	0.039	0.017	0.015	0.008	0.009
benzo[k]fluoranthene	0.359	0.042	0.015	0.023	0.008	0.011
benzo[a]pyrene	0.755	0.040	0.023	0.055	0.018	0.020
indeno[1,2,3-c,d]pyrene	n.d	n.d	n.d	n.d	n.d	n.d
dibenz[a,h]anthracene	n.d	n.d	n.d	n.d	n.d	n.d
benzo[g,h,i]perylene	n.d	n.d	n.d	n.d	n.d	n.d
TOTAL	5.112	1.733	0.839	5.095	0.822	0.823

4. Conclusion

The obtained results showed that the dependence of agronomic properties of biochars on pyrolysis pressure and pyrolysis temperature varied according to the type of feedstock. Nevertheless, no obvious correlations between pyrolysis conditions and biochar properties have been found, indicating that the type of feedstock is a more significant factor. In this study, special focus was given to evaluating the effects of pyrolysis pressure and temperature on PAH concentration. The low-molecular weight PAHs were predominated in all biochars and total PAHs concentration did not exceed the allowed limit set by the EBC. Pyrolysis of biomass having low lignin content yielded biochar with much higher PAH concentrations than that of biomass having high lignin content under identical pyrolysis conditions. Differences in biomass components were also significant in the effect of pyrolysis conditions on total PAH concentration. For example, the temperature and pressure had an effect on PAH concentration in CS-derived biochars, but not for VS-derived biochar.

Acknowledgments This research received funding from the Spanish Research Agency (ref PCIN-2017-048) in the framework of the EU-funded ERANET-MED- 2 Program (project acronym: MEDWASTE).

References

- [1] X. Liu, A. Zhang, C. Ji, S. Joseph, R. Bian, L. Li, G. Pan, J. Paz-Ferreiro, Biochar's effect on crop productivity and the dependence on experimental conditions-a meta-analysis of literature data, *Plant Soil* 373 (2013) 583–594, <https://doi.org/10.1007/s11104-013-1806-x>
- [2] B. Saletnik, G. Zagula, M. Bajcar, M. Tarapatsky, G. Bobula, C. Puchalski, Biochar as a multifunctional component of the environment-a review, *Appl. Sci.* 9 (2019), <https://doi.org/10.3390/app9061139>.
- [3] M. Ji, X. Wang, M. Usman, F. Liu, Y. Dan, L. Zhou, S. Campanaro, G. Luo, W. Sang, Effects of different feedstocks-based biochar on soil remediation: a review, *Environ. Pollut.* 294 (2022), <https://doi.org/10.1016/j.envpol.2021.118655>.
- [4] A.V. Gorovtsov, T.M. Minkina, S.S. Mandzhieva, L.V. Perelomov, G. Soja, I. V. Zamulina, V.D. Rajput, S.N. Sushkova, D. Mohan, J. Yao, The mechanisms of biochar interactions with microorganisms in soil, *Environ. Geochem. Health* 42 (2020) 2495–2518, <https://doi.org/10.1007/s10653-019-00412-5>.
- [5] M. Głodowska, T. Schwinghamer, B. Husk, D. Smith, Biochar based inoculants improve soybean growth and nodulation, *Agric. Sci.* 08 (2017) 1048–1064, <https://doi.org/10.4236/as.2017.89076>.
- [6] Y. Zhang, J. Wang, Y. Feng, The effects of biochar addition on soil physicochemical properties: a review, *Catena* 202 (2021), 105284, <https://doi.org/10.1016/j.catena.2021.105284>.
- [7] A. El-Naggar, A.H. El-Naggar, S.M. Shaheen, B. Sarkar, S.X. Chang, D.C.W. Tsang, J. Rinklebe, Y.S. Ok, Biochar composition-dependent impacts on soil nutrient release, carbon mineralization, and potential environmental risk: a review, *J. Environ. Manag.* 241 (2019) 458–467, <https://doi.org/10.1016/j.jenvman.2019.02.044>.
- [8] M. Hussain, M. Farooq, A. Nawaz, A.M. Al-Sadi, Z.M. Solaiman, S.S. Alghamdi, U. Ammara, Y.S. Ok, K.H.M. Siddique, Biochar for crop production: potential benefits and risks, *J. Soils Sediment.* 17 (2017) 685–716, <https://doi.org/10.1007/s11368-016-1360-2>.
- [9] S.K. Das, G.K. Ghosh, R.K. Avasthe, K. Sinha, Compositional heterogeneity of different biochar: Effect of pyrolysis temperature and feedstocks, *J. Environ. Manag.* 278 (2021), <https://doi.org/10.1016/j.jenvman.2020.111501>.
- [10] J.J. Manya, D. Alvira, M. Videgain, G. Duman, J. Yanik, Assessing the importance of pyrolysis process conditions and feedstock type on the combustion performance of agricultural-residue-derived chars, *Energy Fuels* 35 (2021) 3174–3185, <https://doi.org/10.1021/acs.energyfuels.0c04180>.
- [11] EBC , 2012. 'European Biochar Certificate - Guidelines for a Sustainable Production of Biochar.' European Biochar Foundation (EBC), Arbaz, Switzerland. (<http://european-biochar.org>). Version 9.3E of 11th April 2021.
- [12] W. Song, M. Guo, Quality variations of poultry litter biochar generated at different pyrolysis temperatures, *J. Anal. Appl. Pyrolysis* 94 (2012) 138–145, <https://doi.org/10.1016/j.jaap.2011.11.018>.

- [13] C. Steiner, Considerations in Biochar Characterization, in: 2015: pp. 87–100. <http://doi.org/10.2136/sssaspecpub63.2014.0038.5>.
- [14] K.A. Spokas, Review of the stability of biochar in soils: predictability of O:C molar ratios, *Carbon Manag.* 1 (2010) 289–303, <https://doi.org/10.4155/cmt.10.32>.
- [15] L. Leng, H. Huang, An overview of the effect of pyrolysis process parameters on biochar stability, *Bioresour. Technol.* 270 (2018) 627–642, <https://doi.org/10.1016/j.biortech.2018.09.030>.
- [16] L. Han, K.S. Ro, Y. Wang, K. Sun, H. Sun, J.A. Libra, B. Xing, Oxidation resistance of biochars as a function of feedstock and pyrolysis condition, *Sci. Total Environ.* 617- 617 (2018) 335–344, <https://doi.org/10.1016/j.scitotenv.2017.11.014>.
- [17] J. Lehmann, Stability of biochar in soil, in: S. Joseph (Ed.), *Biochar for Environmental Management. Science and Technology*, Earthscan, London, 2009, pp. 183–205.
- [18] C.H. Liu, W. Chu, H. Li, S.A. Boyd, B.J. Teppen, J. Mao, J. Lehmann, W. Zhang, Quantification and characterization of dissolved organic carbon from biochars, *Geoderma* 335 (2019) 161–169, <https://doi.org/10.1016/j.geoderma.2018.08.019>.
- [19] W. Suliman, J.B. Harsh, N.I. Abu-Lail, A.M. Fortuna, I. Dallmeyer, M. Garcia-Perez, Influence of feedstock source and pyrolysis temperature on biochar bulk and surface properties, *Biomass- Bioenergy* 84 (2016) 37–48, <https://doi.org/10.1016/j.biombioe.2015.11.010>.
- [20] L. Leng, Q. Xiong, L. Yang, H. Li, Y. Zhou, W. Zhang, S. Jiang, H. Li, H. Huang, An overview on engineering the surface area and porosity of biochar, *Sci. Total Environ.* 763 (2021), <https://doi.org/10.1016/j.scitotenv.2020.144204>.
- [21] E. Cetin, R. Gupta, B. Moghtaderi, Effect of pyrolysis pressure and heating rate on radiata pine char structure and apparent gasification reactivity, *Fuel* 84 (2005), 13281334, <https://doi.org/10.1016/J.FUEL.2004.07.016>.
- [22] F. Melligan, R. Auccaise, E.H. Novotny, J.J. Leahy, M.H.B. Hayes, W. Kwapinski, Pressurised pyrolysis of *Miscanthus* using a fixed bed reactor, *Bioresour. Technol.* 102 (2011) 3466–3470, <https://doi.org/10.1016/j.biortech.2010.10.129>.
- [23] A. Tomczyk, Z. Sokołowska, P. Boguta, Biochar physicochemical properties: pyrolysis temperature and feedstock kind effects, *Rev. Environ. Sci. Biotechnol.* 19 (2020) 191–215, <https://doi.org/10.1007/s11157-020-09523-3>.
- [24] M.I. Al-Wabel, A. Al-Omran, A.H. El-Naggar, M. Nadeem, A.R.A. Usman, Pyrolysis temperature induced changes in characteristics and chemical composition of biochar produced from *Conocarpus* wastes, *Bioresour. Technol.* 131 (2013) 374–379, <https://doi.org/10.1016/j.biortech.2012.12.165>.
- [25] A. Hass, J.M. Gonzalez, I.M. Lima, H.W. Godwin, J.J. Halvorson, D.G. Boyer, Chicken manure biochar as liming and nutrient source for acid appalachian soil, *J. Environ. Qual.* 41 (2012) 1096–1106, <https://doi.org/10.2134/jeq2011.0124>.

- [26] B. Glaser, L. Haumaier, G. Guggenberger, W. Zech, The “Terra Preta” phenomenon: a model for sustainable agriculture in the humid tropics, *Naturwissenschaften* 88 (2001) 37–41, <https://doi.org/10.1007/s001140000193>.
- [27] T.T.T. Hien, T. Tsubota, T. Taniguchi, Y. Shinogi, Enhancing soil water holding capacity and provision of a potassium source via optimization of the pyrolysis of bamboo biochar, *Biochar* 3 (2021) 51–61, <https://doi.org/10.1007/s42773-020-00071-1>.
- [28] A.T. Tag, G. Duman, S. Ucar, J. Yanik, Effects of feedstock type and pyrolysis temperature on potential applications of biochar, *J. Anal. Appl. Pyrolysis* 120 (2016) 200–206, <https://doi.org/10.1016/j.jaap.2016.05.006>.
- [29] M.D. Huff, S. Marshall, H.A. Saeed, J.W. Lee, Surface oxygenation of biochar through ozonization for dramatically enhancing cation exchange capacity, *Bioresour. Bioprocess.* 5 (2018), <https://doi.org/10.1186/s40643-018-0205-9>.
- [30] G. Kharel, O. Sacko, X. Feng, J.R. Morris, C.L. Phillips, K. Trippe, S. Kumar, J. W. Lee, Biochar surface oxygenation by ozonization for super high cation exchange capacity, *ACS Sustain. Chem. Eng.* 7 (2019) 16410–16418, <https://doi.org/10.1021/acssuschemeng.9b03536>.
- [31] J.W. Lee, M. Kidder, B.R. Evans, S. Paik, A.C. Buchanan, C.T. Garten, R.C. Brown, Characterization of biochars produced from cornstovers for soil amendment, *Environ. Sci. Technol.* 44 (2010) 7970–7974, <https://doi.org/10.1021/es101337x>.
- [32] J. Lehmann, M.C. Rillig, J. Thies, C.A. Masiello, W.C. Hockaday, D. Crowley, Biochar effects on soil biota - a review, *Soil Biol. Biochem.* 43 (2011) 1812–1836, <https://doi.org/10.1016/j.soilbio.2011.04.022>.
- [33] B. Singh, M.M. Dolk, Q. Shenand, M. Camps-Arbestain, Biochar pH, electrical conductivity and liming potential, in: B. Singh, M. Camps-Arbestain, J. Lehmann (Eds.), *Biochar: A Guide to Analytical Methods*, CSIRO, 2017.
- [34] T. Limwikran, I. Kheoruenromne, A. Suddhiprakarn, N. Prakongkep, R.J. Gilkes, Dissolution of K, Ca, and P from biochar grains in tropical soils, *Geoderma* 312 (2018) 139–150, <https://doi.org/10.1016/j.geoderma.2017.10.022>.
- [35] N. Prakongkep, R.J. Gilkes, W. Wiriyaakitnateekul, Forms and solubility of plant nutrient elements in tropical plant waste biochars, *J. Plant Nutr. Soil Sci.* 178 (2015) 732–740, <https://doi.org/10.1002/jpln.201500001>.
- [36] J.M. De la Rosa, A.M. Sánchez-Martín, P. Campos, A.Z. Miller, Effect of pyrolysis conditions on the total contents of polycyclic aromatic hydrocarbons in biochars produced from organic residues: assessment of their hazard potential, *Sci. Total Environ.* 667 (2019) 578–585, <https://doi.org/10.1016/j.scitotenv.2019.02.421>.
- [37] G. Greco, M. Videgain, C. Di Stasi, E. Pires, J.J. Many`a, Importance of pyrolysis temperature and pressure in the concentration of polycyclic aromatic hydrocarbons in wood waste-derived biochars, *J. Anal. Appl. Pyrolysis* 159 (2021), <https://doi.org/10.1016/j.jaap.2021.105337>.

- [38] W. Buss, M.C. Graham, G. MacKinnon, O. Mašek, Strategies for producing biochars with minimum PAH contamination, *J. Anal. Appl. Pyrolysis* 119 (2016) 24–30, <https://doi.org/10.1016/j.jaap.2016.04.001>.
- [39] H. Zhou, C. Wu, A. Meng, Y. Zhang, P.T. Williams, Effect of interactions of biomass constituents on polycyclic aromatic hydrocarbons (PAH) formation during fast pyrolysis, *J. Anal. Appl. Pyrolysis* 110 (2014) 264–269, <https://doi.org/10.1016/j.jaap.2014.09.007>.
- [40] A. Freddo, C. Cai, B.J. Reid, Environmental contextualisation of potential toxic elements and polycyclic aromatic hydrocarbons in biochar, *Environ. Pollut.* 171 (2012) 18–24, <https://doi.org/10.1016/j.envpol.2012.07.009>.
- [41] R.A. Brown, A.K. Kercher, T.H. Nguyen, D.C. Nagle, W.P. Ball, Production and characterization of synthetic wood chars for use as surrogates for natural sorbents, *Org. Geochem.* 37 (2006) 321–333, <https://doi.org/10.1016/j.orggeochem.2005.10.008>.
- [42] A. Zielinska, P. Oleszczuk, The conversion of sewage sludge into biochar reduces polycyclic aromatic hydrocarbon content and ecotoxicity but increases trace metal content, *Biomass- Bioenergy* 75 (2015) 235–244, <https://doi.org/10.1016/j.biombioe.2015.02.019>.

SUPPLEMENTARY MATERIAL

Table S1. Properties of agricultural wastes [10]

	VS	CS
Proximate Analysis (dry, wt%)		
volatile matter	74.0±1.19	86.6±0.11
fixed carbon	24.9±1.91	10.7±0.49
ash	1.08±0.05	2.70±0.20
Ultimate Analysis (dry, wt%)		
C	47.1±0.14	44.4±0.31
H	5.29±0.09	5.60±0.04
N	0.66±0.05	0.43±0.01
O ^a	47.0	49.6
Component Analysis, (dry, wt%)		
Cellulose	29.3±1.9	40.5±0.9
Hemicellulose	9.26±0.97	21.4±0.5
Lignin	19.2±1.4	9.68±0.50
Extractives	4.54±0.37	8.94±0.77

^a calculated from difference

Table S2. Chemical Composition of Biomass Ashes [10]

	VS	CS
CaO	58.3±0.25	30.7±0.23
K ₂ O	18.4±0.12	9.85±0.15
MgO	6.66±0.14	3.45±0.17
SiO ₂	5.73±0.08	31.4±0.23
Fe ₂ O ₃	3.51±0.11	6.49±0.12
P ₂ O ₅	1.24±0.06	4.13±0.10
Al ₂ O ₃	2.57±0.07	4.85±0.12
PbO	1.24±0.04	4.13±0.10
S (inorganic)	0.26±0.02	2.50±0.08
Cl (inorganic)	0.48±0.02	0.59±0.03
MnO	0.53±0.03	0.53±0.03
ZnO	0.32±0.02	0.24±0.02
SnO ₂	0.26±0.02	0.45±0.03
TiO ₂	0.34±0.02	0.59±0.03